STUDY OF THE EFFECT OF A POLYPYRROLE COATING OBTAINED BY ELECTROPOLYMERIZATION ON THE CORROSION BEHAVIOR OF ASTM F1586 SURGICAL STAINLESS STEEL

Camila Boldrini Nascimento, camila.boldrini@ufabc.edu.br **1**
Renato Altobelli Antunes, renato.antunes@ufabc.edu.br **1**
Everaldo Carlos Venâncio , everaldo.venancio@ufabc.edu.br **1**

[1]Universidade Federal do ABC (UFABC), Centro de Engenharia, Modelagem e Ciências Sociais Aplicadas (CECS), 09210 580 Santo André, SP, Brazil

Abstract. *Conductor polymeric films can act as anodic inhibitors, accelerating and stabilizing the formation of protective oxide films on metallic materials. Polypyrrole is a conducting polymer with good chemical stability, wide range of electrical conductivity, low cost and simple synthesis. In the present work, a polymeric polypyrrole coating was deposited by electropolymerization on the surface of a ASTM F1586 surgical stainless steel. The objective was to investigate the effect of the polypyrrole layer on the corrosion behavior of the ASTM F1586 steel. The caracterization of the electrochemical behavior was made by electrochemical impedance spectroscopy and potentiodynamic polarization. The tests were conducted on PBS (phosphate buffered solution) at 37ºC. The morphology of the layer was evaluated by scanning electron microscopy and surface roughness was analysed by confocal laser scanning microscopy. The results showed the formation of a homogeneous film. The EIS tests indicated electrolyte penetration through the polypyrrole layer. However, the corrosion current density was decreased when compared to the bare substrate.*

Keywords: *surgical stainless steel, polypyrrole coating, conducting polymer film, corrosion.*

1. INTRODUCTION

AISI 316L austenitic stainless steel grades have been widely employed for biomedical devices due to a combination of good mechanical strength, high toughness, ease of manufacturing and low cost when compared to other metallic biomaterials (GOPI, RAMYA, RAJESWARI, & KAVITHA, 2013). Corrosion resistance derives from the formation of a passive oxide film on its surface which is composed of Cr and Fe hydrated oxides. This oxide layer is continuous, thin and compact, consisting in a barrier between the metal surface and the physiological medium. Yet, even in the presence of the passive film, metallic ions are released, reaching neighboring tissues next to the stainless steel component. Nickel ions, for instance, can promote allergenic reactions *in vivo* (GOPI, RAJESWARI, et al., 2013).

In order to optimize the corrosion resistance of austenitic stainless steel biomaterials the ASTM F1586 (ISO 5832-9) grade has been developed. This material has high nitrogen content to stabilized the austenitic phase and reduced nickel content with respect to the conventional AISI 316L composition, surpassing its corrosion stability (ARAUJO, 2004). Nickel content reduction enables diminishing allergenic reaction caused by the contact between the biomedical device and the human tissues. Moreover, superior Mo and Cr contents imply in further corrosion stability. The low sulfur and phosphorus contents increase fatigue strength with respect to the AISI 316L stainless steel (BUSS, 2011). However, in spite of the optimized chemical composition, the ASTM F1586 grade is prone to pitting and crevice in the human body.

Conductive polymer films can be deposited on stainless steels to increase their corrosion resistance. Polyaniline (PANI) and polypyrrole (PPy) conductive polymer films are reported as protective coatings for stainless steel substrates (GOPI, RAMYA, et al., 2013). These films can act either as barrier layer or anodic inhibitors, accelerating the formation of protective oxides on the metallic surface. Polypyrrole coatings are reported to present good chemical stability, low cost and are easily synthesized (BALINT, CASSIDY, & CARTMELLl, 2014).

In this work, PPy films were obtained by electropolymerization on the surface of ASTM F1586 specimens. The film morphology and roughness were examined using scanning electron microscopy and confocal laser scanning microscopy, respectively. The corrosion resistance was evaluated in phosphate buffered saline (PBS) solution by electrochemical impedance spectroscopy measurements and potentiodynamic polarization tests.

2. EXPERIMENTAL PROCEDURE

ASTM F1586 cylindrical bar was kindly provided by Villares Metals. The dimensions of the as-received material were 170 mm (length) and 15 mm (diameter). Its nominal chemical composition is shown in Tab. 1.

Table 1. Nominal chemical composition of the ASTM F1586 stainless steel.

Element	C	Mn	P	S	Si	Cr	Ni	Mo	N	Nb	Cu
Wt.%	0.08	2.0-4.25	0.025	0.01	0.075	19.5 – 22.0	9.0 – 11.0	2 -3	0.25 – 0.5	0.25 – 0.8	0.25

2.1 Sample preparation

Samples for the electrochemical tests were cut from the as-received round bar using a precision metallographic cutter (Isomet 4000) equipped with a diamond wafering blade. Small pieces with flat surface area of approximately 0.45 cm2 were obtained. A copper wire was, then, glued to the rear surface by means of a coloidal conductive silver paste. Next, this set was embedded in cold-curing epoxy resin. After complete curing, the specimens were ground using SiC emery papers with progressively finer grain sizes up to grit 2400. Surface finishing was finally accomplished by subsequent polishing with alumina abrasive paste (6 μm). Next, the polished specimens were washed with distilled water and dried at ambient air.

2.2 Polypyrrole (PPy) coating deposition

Electropolymerization of PPy films was carried out by cyclic voltammetry. The ASTM F1586 substrates were placed in a glass cell. The deposition procedure was based on a conventional three-electrode cell setup, using a platinum wire as the counter-electrode, Ag/AgCl as reference and the stainless steel specimen as the working electrode. The potential was scanned from -0.53 $V_{Ag/AgCl}$ up to +1.47 $V_{Ag/AgCl}$ at a sweep rate of 20 $mV.s^{-1}$ for 60 cycles. The electrolyte consisted of 0.5 M sodium salicylate and 0.1 M polypyrrole solution at room temperature. High purity nitrogen was continuously bubbled into the glass cell during electropolymerization to avoid oxygen contamination. The tests were conducted in triplicate using a potentiostat/galvanostat Autolab M101. After deposition, the specimens were washed with distilled water and dried in ambient air.

2.3 Electrochemical tests

The corrosion behavior of PPy-coated ASTM F1586 specimens was evaluated in PBS solution at 37 °C provided by a microprocessor controlled water bath. The tests were performed in a conventional three-electrode cell configuration, using a platinum wire as the auxiliary electrode, Ag/AgCl as reference and the coated specimens as the working electroless. The experimental setup consisted of an initial monitoring of the open circuit potential (OCP) for 1 h in order to ensure a steady-state condition. Next, EIS measurements were carried out at the OCP in the frequency range from 100 kHz to 10 mHz, amplitude of the sinusoidal perturbation signal of ±10 mV (rms) at an acquisition rate of 10 points per decade. Potentiodynamic polarization tests were conducted right after the EIS measurements by sweeping the potential from -300 mV versus the OCP up to +1.0 $V_{Ag/AgCl}$ at a scan rate of 1 $mV.s^{-1}$. The tests were performed in triplicate using an Autolab M101 potentiostat/galvanostat.

2.4 Surface characterization

The surface morphogy of the electropolymerized PPy films was examined using scanning electron microscopy (Hitachi TM3000). Surface roughness was evaluated by confocal laser scanning microscopy (Olympus LEXT OLS4100). The results are expressed as the Ra parameter (average surface roughness).

3. RESULTS AND DISCUSSION

3.1 Surface morphology and roughness

Figure 1 shows a SEM micrograph of the PPy-coated ASTM F1586 stainless steel. The PPy film was homogeneously deposited on the substrate. However, surface defects can be perceived as indicated by the small darker areas distributed within the brighter matrix. These defects are inherent to the electropolymerization deposition process. The electrochemical response of the coated electrode can be affected by the surface defects. Indeed, defective sites are preferential paths for electrolyte penetration through coated metals, being related to faster dissolution rates with respect to the uncoated substrate (ZHUANG et al., 2015). The surface morphology of PPy films can be affected by electropolymerization. Al-Jaouhari et al. obtained PPy coatings with a typical globular morphology (Cauliflower aspect) on carbon steel substrates, using galvanostatic control at a current density of 5 mA.cm^{-2} (EL JAOUHARI et al., 2017). Gopi et al. obtained an agglomerated, granular and uniform PPy layer on 316L stainless steel substrates using cyclic voltammetry. Our results point to a smoother surface, permeated by several microscopic defects (GOPI, RAJESWARI, et al., 2013).

Surface roughness was determined using CLSM. Figure 2 shows 2D and 3D micrographs of the PPy-coated ASTM F1586 stainless steel obtained by CLSM. The surface is relatively smooth. The Ra value was determined as 2.68±0.38 µm. Roughness is often reported to influence the corrosion behavior of metallic surfaces. The presence of high peaks and deep valleys (rough surface) is frequently associated with fast corrosion kinetics (ZUO, WANG, & XIONG, 2002).

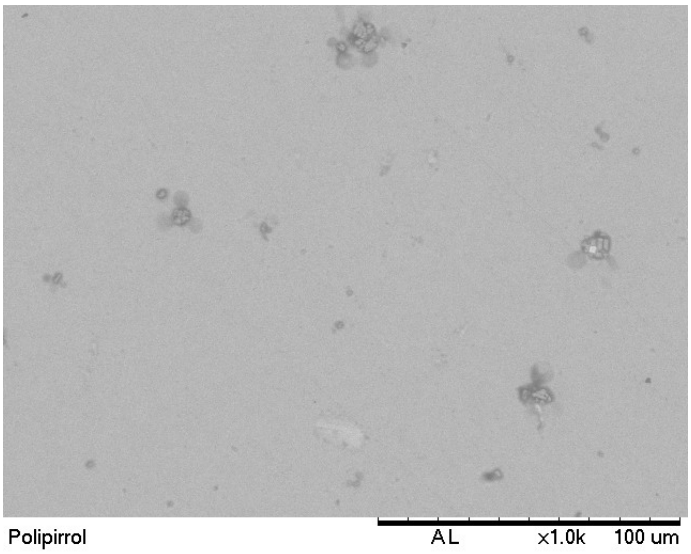

Figure 1. SEM micrograph of the PPy-coated ASTM F1586 stainless steel.

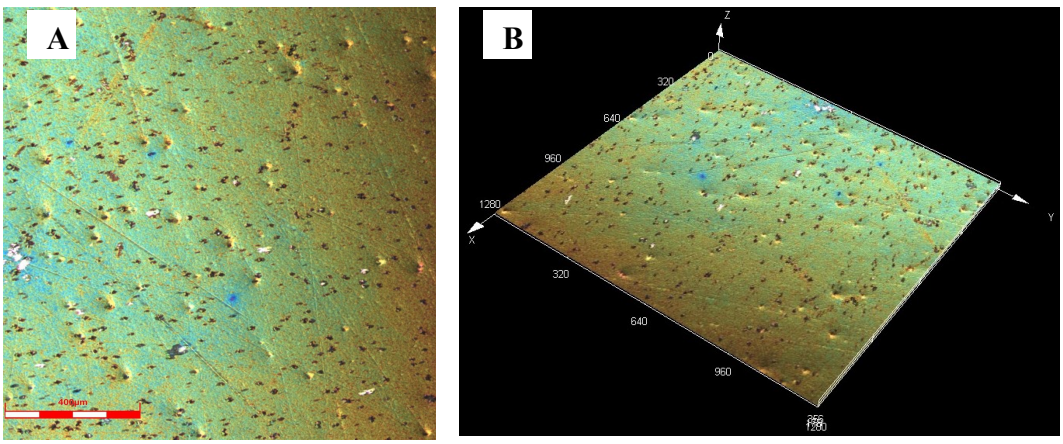

Figure 2. CLSM micrographs of the PPy-coated ASTM F1586 stainless steel: a) 2D and b) 3D views.

3.2 EIS measurements

EIS diagrams of the PPy-coated and uncoated ASTM F1586 stainless steel are shown in Fig. 3. The tests were conducted in PBS solution at 37°C, after 1 h of immersion. Nyquist plots (Fig. 3a) are characterized by a capacitive loop whose diameter is lower for the PPy-coated substrate when compared to the uncoated sample. The diameter of the capacitive semicircle is associated with the corrosion resistance of the electrode surface (OLIVEIRA, AGUIAR, VAZQUEZ, ROBIN, & BARBOZA, 2014). In this respect, the defective sites of the PPy layer (Fig. 1) are likely to decrease the capacitive behavior of the coated metal when compared to the bare substrate. This effect is also observed in the Bode plots. Phase plots (Fig. 3b) present one single time constant as suggested by the presence of one shoulder extending from the middle to the low frequency domain. The phase angle reaches -80° for the uncoated substrate and remains near this value through a wider frequency range than the PPy-coated before decreasing at low frequencies. The phase angle drop at low frequencies is associated with charge transfer reactions, being related to corrosion processes taking place the electrode surface (XU, ZHANG, LUO, JIN, & ZHANG, 2013). Bode log $|Z|$ vs. log f plots are typically capacitive, showing a slope of approximately -1 (ANTUNES et al., 2016) from the middle to the low frequency domain. The PPy-coated sample deviates from the capacitive behavior at the lowest frequencies. The higher impedance modulus of the uncoated material at the lowest frequencies is also an indication of its reduced corrosion susceptibility.

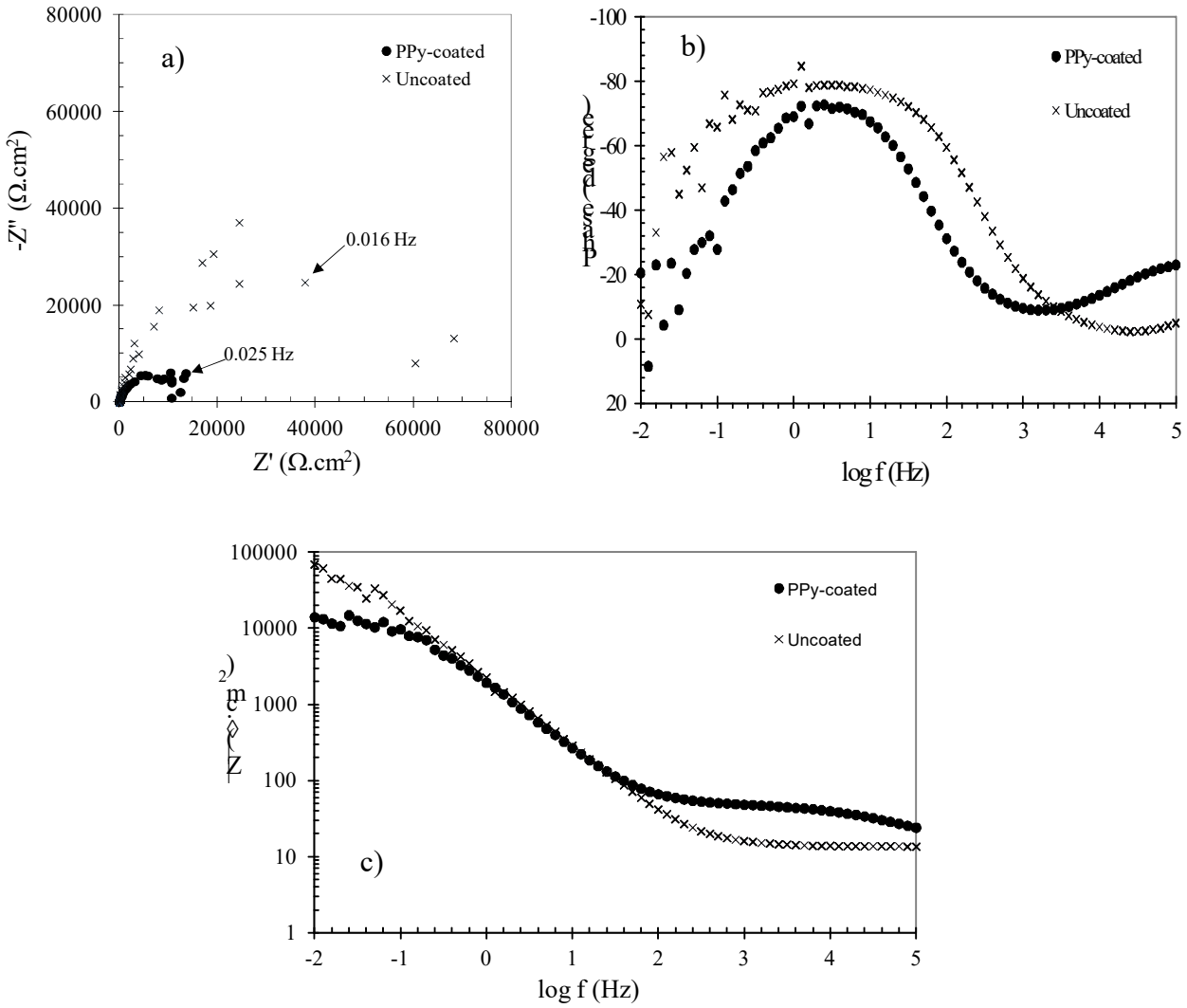

Figure 3. EIS diagrams of the PPy-coated and uncoated ASTM F1586 stainless steel: a) Nyquist plots; b) Bode – Phase plots; c) Bode – impedance modulus plots. Data obtained in PBS solution at 37°C.

3.3 Potentiodynamic polarization

Potentiodynamic polarization curves of the PPy-coated and uncoated ASTM F 1586 stainless steel are shown in Fig. 4. The tests were carried out right after the EIS measurements. The values of corrosion potential (E_{corr}) are displayed in Tab. 1. The passive current densities (i_p) were also determined. As the polarization curves do not indicate active control in the anodic branches, the values of corrosion current densities were not determined, since, in this case, the corrosion kinetics is given by the passive current density (MCCAFERTY, 2010).

The potentiodynamic polarization curves are typically passive, showing a wide potential range throughout the anodic branch where the current density remains nearly constant. The corrosion potential (E_{corr}) of the PPy-coated steel was shifted to more anodic value in comparison with the uncoated substrate. This effect was also observed by González and Saidman (2012) for a polypyrrole film electropolymerized onto the surface of 316L stainless steel specimens, being explained by an anodic protection mechanism. The value of E_{corr} is associated with the electrode surface activity (ABOU-KRISHA, ASSAF, & EL-NABY, 2016). The conductive polymer topcoat decreased the thermodynamic activity of the ASTM F1586 surface. Notwithstanding, EIS data indicate that the PPy layer is not immune to electrolyte penetration. In this respect, surface morphology seems to play a central role in the corrosion protection ability of the as-deposited film.

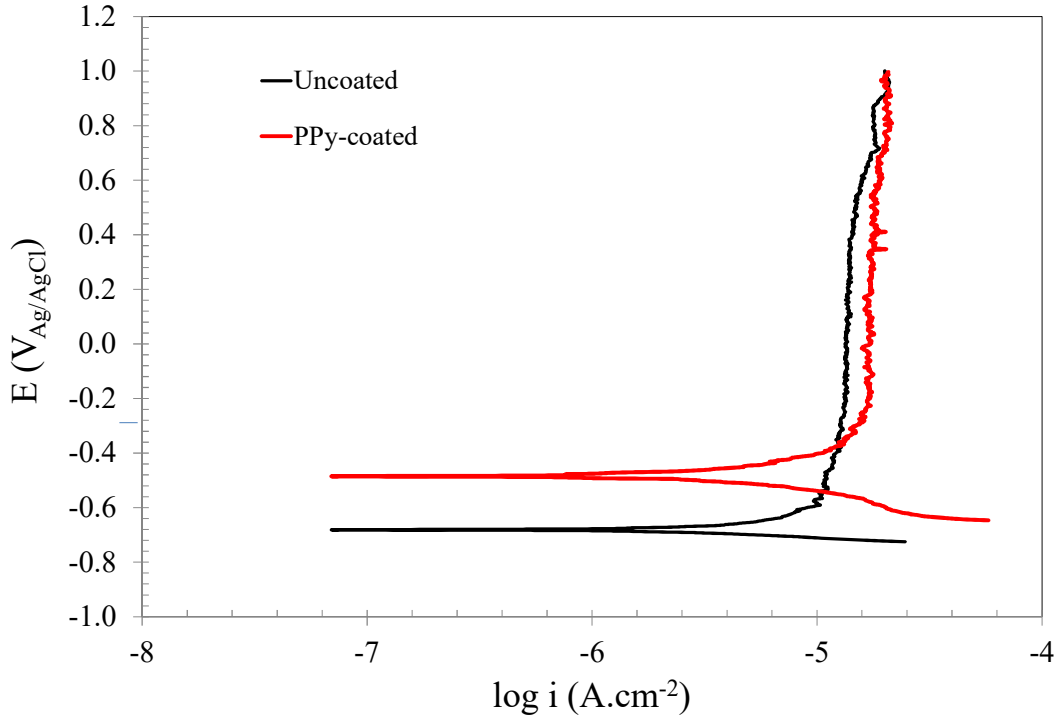

Figure 4. Potentiodynamic polarization curves of the PPy-coated and uncoated ASTM F1586 stainless steel in PBS solution at 37°C.

Table 1. Electrochemical parameters determined from the potentiodynamic polarization curves.

Sample	E_{corr} *(V)*	i_p *(µA.cm^{-2})*
PPy-coated	-0.49	17.4
Uncoated	-0.68	13.5

The onset of pitting corrosion was not perceived in the polarization curves. The passive range extends up to the end of the test either for the PPy-coated or uncoated substrates. The passive current density (i_p) values were determined and are displayed in Tab. 1. This parameter can be associated with the electrode dissolution rate. In spite of the similarity between both conditions, the uncoated sample presented lower ip, suggesting that the PPy coating did not offer an effective barrier against substrate dissolution. This result is in agreement with the EIS data and can be due to the defective sites observed in the SEM micrograph shown in Fig. 1.

5. CONCLUSÕES

PPy coatings were successfully obtained by electropolymerization on the surface of ASTM F1586 stainless steel specimens. The surface morphology indicates the formation of a uniform and smooth layer, permeated by several defects. The PPy layer was smooth with an average roughness of Ra = 2.68 μm.

The corrosion resistance of the PPy-coated substrate was affected by the film defects, as indicated by EIS and potentiodynamic polarization tests. The impedance values of the coated surface were lower than those of the uncoated substrate, suggesting that electrolyte penetration throughout the coating defects can take place, thus hampering the corrosion protection ability of the PPy layer. The corrosion kinectics of the PPy-coated steel was slightly faster than that of the bare substrate, as indicated by the passive current densities. This effect was also related to the surface morphology of the as-deposited layer. In spite of the anodic shift of the corrosion potential after PPy deposition, our results suggest that the electropolymerization procedure need to be optimized to obtain a more compact, defect-free layer. Varying the pyrrole monomer concentration in the electropolymerization solution and the use of galvanostatic control during deposition can be alternatives to enhance the corrosion properties of the PPy layer.

6. ACKNOWLEDGMENTS

The authors are thankful to Villares Metals for kindly providing the material used in the presente work and CAPES for the financial support.

7. REFERENCES

ABOU-KRISHA, M. M., ASSAF, F. H., & EL-NABY, S. A. (2016). The influence of Fe2+ concentration and deposition time on the corrosion resistance of the electrodeposited zinc–nickel–iron alloys. *Arabian Journal of Chemistry, 9, Supplement 2*, S1349-S1356. doi: http://dx.doi.org/10.1016/j.arabjc.2012.02.014

ANTUNES, R. A., DE OLIVEIRA, M. C. L., PILLIS, M. F., GERIBOLA, G. A., SCHEIDT, G., & DE ARAUJO, E. G. (2016). Corrosion of thin, magnetron sputtered Nb2O5 films. *Corrosion Science, 102*, 317-325. doi: http://dx.doi.org/10.1016/j.corsci.2015.10.023

ARAUJO, T. L. C., A.A. (2004). Estudo do aço inoxidável aplicado como implante ortopédico. *Revista Mackenzie*.

BALINT, R., CASSIDY, N. J., & CARTMELLl, S. H. (2014). Conductive polymers: Towards a smart biomaterial for tissue engineering. *Acta Biomaterialia, 10*(6), 2341-2353. doi: http://dx.doi.org/10.1016/j.actbio.2014.02.015

BUSS, G. A. M. D., K. S; VICENTE, M.G. (2011). Utilização de aços inoxidáveis em implantes. *BIT – Boletim Informativo de Tecnovigilância, Brasília.*

EL JAOUHARI, A., EL ASBAHANI, A., BOUABDALLAOUI, M., AOUZAL, Z., FILOTÁS, D., BAZZAOUI, E. A., . . . HARTMANN, D. (2017). Corrosion resistance and antibacterial activity of electrosynthesized polypyrrole. *Synthetic Metals, 226*, 15-24. doi: http://dx.doi.org/10.1016/j.synthmet.2017.01.008

GOPI, D., RAJESWARI, D., RAMYA, S., SEKAR, M., PRAMOD, R., DWIVEDI, J., . . . RAMASESHAN, R. (2013). Enhanced corrosion resistance of strontium hydroxyapatite coating on electron beam treated surgical grade stainless steel. *Applied Surface Science, 286*, 83-90. doi: http://dx.doi.org/10.1016/j.apsusc.2013.09.023

GOPI, D., RAMYA, S., RAJESWARI, D., & KAVITHA, L. (2013). Corrosion protection performance of porous strontium hydroxyapatite coating on polypyrrole coated 316L stainless steel. *Colloids and Surfaces B: Biointerfaces, 107*, 130-136. doi: http://dx.doi.org/10.1016/j.colsurfb.2013.01.065

MCCAFERTY, E. (2010). *Introduction to Corrosion Science*. NY, USA: Springer.

OLIVEIRA, V. M. C. A., AGUIAR, C., VAZQUEZ, A. M., ROBIN, A., & BARBOZA, M. J. R. (2014). Improving corrosion resistance of Ti–6Al–4V alloy through plasma-assisted PVD deposited nitride coatings. *Corrosion Science, 88*, 317-327. doi: http://dx.doi.org/10.1016/j.corsci.2014.07.047

XU, A., ZHANG, F., LUO, B., JIN, F., & ZHANG, T. (2013). Investigation the Deterioration Process of Organic Coating Using Changing Rate of Phase Angle at High Frequency United to Neural Network. *International Journal of Electrochemical Science, vol. 8*, p. 773 - 779.

ZHUANG, Y., JIANG, X., ROGACHEV, A. V., PILIPTSOU, D. G., YE, B., LIU, G., . . . RUDENKOV, A. S. (2015). Influences of pulse frequency on the structure and anti-corrosion properties of the a-C:Cr films. *Applied Surface Science, 351*, 1197-1203. doi: http://dx.doi.org/10.1016/j.apsusc.2015.05.157

ZUO, Y., WANG, H., & XIONG, J. (2002). The aspect ratio of surface grooves and metastable pitting of stainless steel. *Corrosion Science, 44*(1), 25-35. doi: http://dx.doi.org/10.1016/S0010-938X(01)00039-7